[10]Huang, Y., Xia, X. L., and Tan, H. P., "Comparison of Two Methods for Solving Radiative Heat Transfer in a Graded Index Semitransparent Slab," *Numerical Heat Transfer, Part B*, Vol. 44, No. 1, 2003, pp. 83–99.

Two-Dimensional Hyperbolic Heat Conduction with Temperature-Dependent Properties

W. Shen* and S. Han†
Tennessee Technological University, Cookeville, Tennessee 38505

Nomenclature

c_p	=	specific heat at constant pressure
k	=	thermal conductivity
P	=	period of on–off heat flux
$q_{x(y)}$	=	$x(y)$ direction heat flux
T	=	temperature
Tr	=	reference temperature
t	=	time
α	=	thermal diffusivity $(k/\rho C_p)$
κ	=	fraction of period P
ρ	=	density
τ	=	relaxation time (α/c^2)

Introduction

THE phenomena of non-Fourier heat conduction are observed in many industrial applications, such as laser heating, cryogenic engineering, and nanotechnology. Various conduction models have been proposed to explain the non-Fourier conductive heat-transfer behavior in a very short period of time. These include the macro-hyperbolic model[1] and Tzou's dual-phase model.[2] The purpose of the present work is to present a numerical solution to the macrohyperbolic heat-conduction (HHC) model in temperature-dependent materials. Both the analytical[3] and numerical[4–8] methods have been used in solving HHC equation over the years. Glass et al.[4] studied the effects of temperature-dependent thermal conductivity on the thermal wave propagation by using the MacCormack's predictor-corrector scheme. Kar et al.[5] solved a nonlinear HHC equation both analytically and numerically by using the Kirchhoff transformation to linearize the nonlinear terms. However, only one-dimensional problems were considered in their works.[4,5] Present numerical approach employs the Roe–Sweby's total-variation-diminishing (TVD)[9] scheme to solve two-dimensional HHC equations. This scheme was used in a previous study for HHC in composite media.[7] The present work investigates the effects of temperature-dependent properties on the thermal wave propagation in a homogeneous medium.

Mathematical Formulations and Numerical Method

The same form of governing equations of HHC is used in this paper as shown in a Ref. 8, which includes an energy equation and two heat-flux equations:

$$\frac{\partial T}{\partial t} + \frac{1}{\rho C_p}\frac{\partial q_x}{\partial x} + \frac{1}{\rho C_p}\frac{\partial q_y}{\partial y} = \frac{s}{\rho C_p} \tag{1a}$$

$$\frac{\partial q_x}{\partial t} + \frac{k}{\tau}\frac{\partial T}{\partial x} = -\frac{q_x}{\tau} \tag{1b}$$

$$\frac{\partial q_y}{\partial t} + \frac{k}{\tau}\frac{\partial T}{\partial y} = -\frac{q_y}{\tau} \tag{1c}$$

It is assumed that τ remains constant, while k, α, ρ, and C_p change with temperature. Because $\alpha = k/\rho C_p$, the influences of ρ and C_p can be included in the ratio of α/k. With the assumption of $k = k_0(1+\beta T)$ and $\alpha/k = \alpha_0/k_0(1+\gamma T)$, the effect of k on the thermal wave propagation can be observed by changing the value of β, and the combined effects of α, ρ, and C_p on the thermal wave propagation can be obtained by varying the value of γ. Equation (1) is nondimensionalized, and the detailed procedure of nondimensionalization can be seen in a Ref. 8. After nondimensionalization, the equations can be written in a vector form as

$$\frac{\partial \boldsymbol{U}}{\partial t} + \frac{\partial \boldsymbol{E}}{\partial x} + \frac{\partial \boldsymbol{F}}{\partial y} = \boldsymbol{S} \tag{2}$$

where

$$\boldsymbol{U} = [T, q_x, q_y]^T, \qquad \boldsymbol{E} = [(1+\gamma T)q_x, (1+0.5\beta T)T, 0]^T$$

$$\boldsymbol{F} = [(1+\gamma T)q_y, 0, (1+0.5\beta T)T]^T$$

$$\boldsymbol{S} = [(1+\gamma T)(s/2), -2q_x, -2q_y]^T$$

Equation (2) is transformed from the Cartesian coordinates to the computational coordinates (ξ, η) and is solved by a fractional step method of Roe–Sweby's TVD scheme.[9] This scheme is second-order accurate in the smooth region and first order in the vicinity of discontinuities:

$$\boldsymbol{U}^*_{j,k} = \boldsymbol{U}^n_{j,k} - (\Delta t/\Delta\xi)J_{j,k}\left(\bar{\boldsymbol{E}}^n_{j+\frac{1}{2},k} - \bar{\boldsymbol{E}}^n_{j-\frac{1}{2},k}\right) + \tfrac{1}{2}(\Delta t/\Delta\xi)J_{j,k}\bar{\boldsymbol{S}}^n_{j,k} \tag{3a}$$

$$\boldsymbol{U}^{n+1}_{j,k} = \boldsymbol{U}^*_{j,k} - (\Delta t/\Delta\eta)J_{j,k}\left(\bar{\boldsymbol{F}}^*_{j,k+\frac{1}{2}} - \bar{\boldsymbol{F}}^*_{j,k-\frac{1}{2}}\right) + \tfrac{1}{2}(\Delta t/\Delta\eta)J_{j,k}\bar{\boldsymbol{S}}^*_{j,k} \tag{3b}$$

where J is the Jacobian matrix. A more detailed description on the computational steps is presented elsewhere.[8]

Results and Conclusion

Example 1: Rectangular Cavity with Linear Boundary Conditions

The first example is a rectangular cavity with insulated top and bottom boundaries. A grid system of 400×40 control volumes is used, which gives a grid-independent solution, and Courant–Friedrichs–Lewy is kept at a constant value of 0.5. The dimensionless temperature in the rectangular cavity is initially 1.0 everywhere, and there is no heat generation inside the rectangular cavity. For time $t > 0$, a periodic on–off heat flux is supplied to the left boundary ($\xi = 0$), and the dimensionless temperature at the right boundary ($\xi = 1$) is kept at 1.0. The periodic on–off heat flux is prescribed by[6]

$$f(t) = \begin{cases} 1.0 & (i-1)P < t < [(i-1)+\kappa]P \\ 0 & [(i-1)+\kappa]P < t < iP \qquad i = 1, 2, 3, \ldots \end{cases} \tag{4}$$

where i represents the number of periods and P is the period. Here we choose $\kappa = 0.5$ and $P = 0.1$.

The effect of k on the thermal wave propagation can be observed by changing the value of β, and the combined effects of α, ρ, and C_p on the thermal wave propagation can be obtained by varying the value of γ. The influences of β and γ on the thermal wave propagation are plotted in Figs. 1 and 2, respectively at $t = 0.8$.

Received 17 July 2003; revision received 13 November 2003; accepted for publication 14 November 2003.

*Graduate Student, Department of Mechanical Engineering; currently Ph.D. Candidate, Department of Computer Science, The University of Kentucky.
†Professor, Department of Mechanical Engineering. Member AIAA.

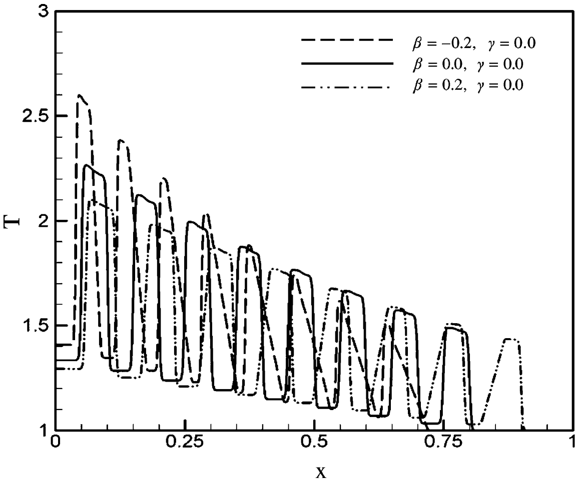

Fig. 1 Influence of β alone on temperature distribution.

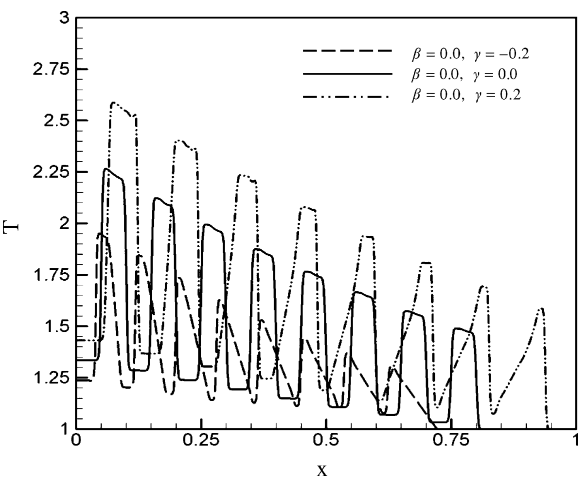

Fig. 2 Influence of γ alone on temperature distribution.

To compare our two-dimensional solution with the published one-dimensional results, the top and bottom boundaries are insulated. It can be seen from Fig. 1 that with a constant heat flux at the left boundary a positive value of β increases the wave speed but lowers the temperature amplitude, whereas a negative β decreases the wave speed but raises the temperature amplitude. Glass et al.[4] reported a similar phenomenon in their one-dimensional nonlinear HHC calculation, where a single pulse of energy was supplied at the left boundary. In their results, numerical oscillations appeared on both sides of thermal wave. Unlike their solution, no numerical oscillations are observed in the vicinity of the discontinuities in the present results as shown in Fig. 1.

Figure 2 shows the effect of γ on the thermal wave propagation at $t = 0.8$. When $\gamma = 0.2$, the wave speed increases, and so does the temperature amplitude. When $\gamma = -0.2$, the wave speed decreases, and the temperature amplitude decreases too. The influence of β and γ on the wave speed agrees with physical expectation because the wave propagates with a speed of $\sqrt{[(\xi_x^2 + \xi_y^2)(1 + \gamma T)(1 + \beta T)]}$. It can be noticed that when either β or γ is negative the sharp discontinuities appear in the rear of the wave, while temperature changes gradually in the front of the wave; when either β or γ is positive, the sharp discontinuities appear in the front of the wave, while temperature changes gradually in the rear of the wave. It is clear that the nonlinear nature caused by the temperature-dependent properties has significant influence on the wave length, wave speed, and wave profile in HHC.

Example 2: Converging–Diverging Cavity with Nonlinear Boundary Conditions

The second example examines the effects of radiative boundary condition on the thermal wave propagation in HHC. In this example, a converging–diverging cavity is investigated. A grid system of 200×100 control volumes is used with a fixed Courant number of 0.5. With the surface radiation at the left boundary, the heat flux to the medium at the left boundary is greatly reduced, and the surface temperature remains very low. To observe the thermal wave propagation more clearly, the boundary heat flux is increased from $f(t) = 1.0$ to $f(t) = 2.0$ when $(i-1)P < t < [(i-1) + \kappa]P$ in Eq. (4).

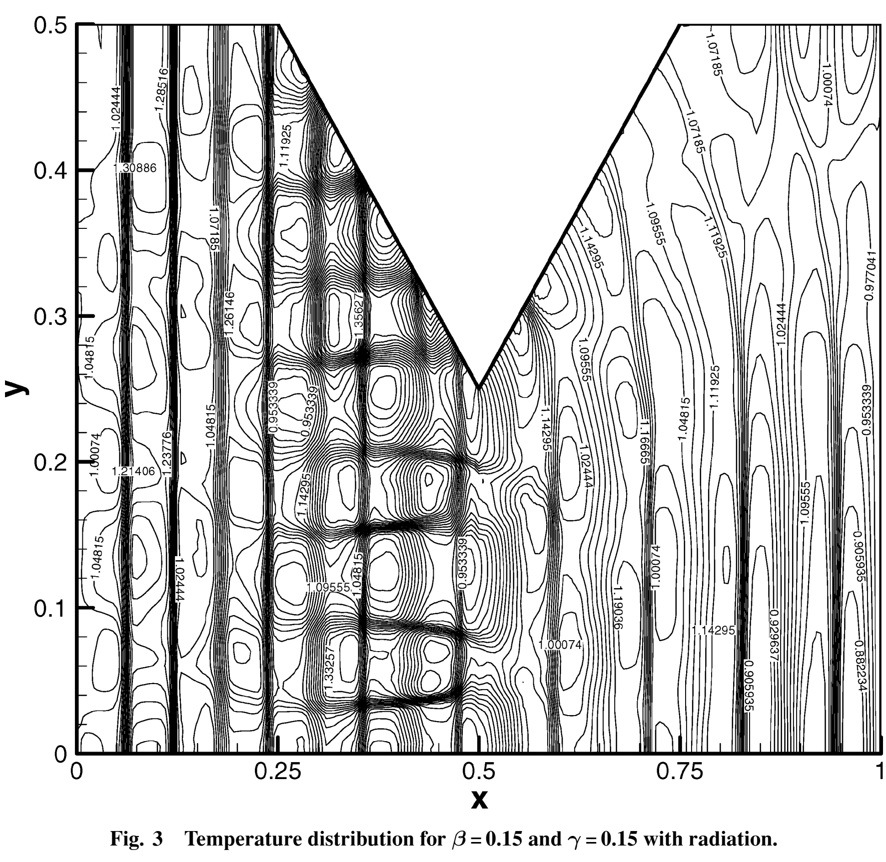

Fig. 3 Temperature distribution for $\beta = 0.15$ and $\gamma = 0.15$ with radiation.

The radiative boundary condition at $\xi = 0$ can be written as

$$q_{\xi} = \varepsilon\sigma\left(T_{\infty}^{4} - T^{4}\right) + f(t) \tag{5}$$

Equation (5) is nondimensionalized and is combined with an energy balance equation at the left boundary to calculate the boundary temperature as follows:

$$k\left(T_{1,k}^{n+1^4} - T_{\infty}^{4}\right) + \left(T_{1,k}^{n+1} - 2J_{1,k}W_{1,k,A}^{3,n+1}\right)\frac{\sqrt{1+\beta T_{1,k}^{n+1}}}{\sqrt{1+\gamma T_{1,k}^{n+1}}} - f(t) = 0 \tag{6}$$

where W is the characteristics. Newton's iteration method is used to calculate temperature $T_{1,k}^{n+1}$ from Eq. (6). For simplicity of presentation, $T_{\infty} = 0$ and $k = 1.0$ are assumed.

The effect of surface radiation on the thermal wave propagation is displayed in Fig. 3. For brevity, only the result of $\beta = 0.15$ and $\gamma = 0.15$ at $t = 1$ is presented. A comparison between the numerical results with and without (not shown) surface radiation shows that the surface radiation does not change the speed of the thermal wave propagation and reflection but greatly decreases the wave strength.

References

[1]Cattaneo, C., "A Form of Heat Conduction Equations Which Eliminates the Paradox of Instantaneous Propagation," *Compte Rendus*, Vol. 247, No. 4, 1958, pp. 431–433.

[2]Tzou, D. Y., "A Unified Field Approach for Heat Conduction from Macro- to Micro-Scales," *Journal of Heat Transfer*, Vol. 117, Feb. 1995, pp. 8–16.

[3]Baumeister, K. J., and Hamill, T. D., "Hyperbolic Heat Conduction Equation—A Solution for the Semi-Infinite Body Problem," *Journal of Heat Transfer*, Vol. 91, Nov. 1969, pp. 543–548.

[4]Glass, D. E., Özisik, M. N., McRae, D. S., and Vick, B., "Hyperbolic Heat Conduction with Temperature-Dependent Thermal Conductivity," *Journal of Applied Physics*, Vol. 59, No. 6, 1986, pp. 1861–1865.

[5]Kar, K., Chan, C. L., and Mazumder, J., "Comparative Studies on Nonlinear Hyperbolic and Parabolic Heat Conduction for Various Boundary Conditions: Analytic and Numerical Solutions," *Journal of Heat Transfer*, Vol. 114, Feb. 1992, pp. 14–20.

[6]Yang, H. Q., "Characteristic-Based, High Order Accurate and Non-Oscillatory Numerical Method for Hyperbolic Heat Conduction," *Numerical Heat Transfer (Part B)*, Vol. 18, 1990, pp. 221–241.

[7]Shen, W., and Han, S., "Hyperbolic Heat Conduction in Composite Materials," AIAA Paper 2002-3003, June 2002.

[8]Shen, W., and Han, S., "An Explicit TVD Scheme for Hyperbolic Heat Conduction in Complex Geometry," *Numerical Heat Transfer (Part B)*, Vol. 41, No. 6, 2002, pp. 565–590.

[9]Tannehill, J. C., Anderson, D. A., and Pletcher, R. H., *Computational Fluid Mechanics and Heat Transfer*, 2nd ed., Taylor and Francis, Washington, DC, 1997, pp. 207–217.